nature nanotechnology

LETTERS

PUBLISHED ONLINE: 14 NOVEMBER 2010 | DOI: 10.1038/NNANO.2010.215

Atomic-scale engineering of electrodes for single-molecule contacts

Guillaume Schull[1]*, Thomas Frederiksen[2]*, Andrés Arnau[2,3,4], Daniel Sánchez-Portal[2,3] and Richard Berndt[5]

The transport of charge through a conducting material depends on the intrinsic ability of the material to conduct current and on the charge injection efficiency at the contacts between the conductor and the electrodes carrying current to and from the material[1-3]. According to theoretical considerations[4], this concept remains valid down to the limit of single-molecule junctions[5]. Exploring this limit in experiments requires atomic-scale control of the junction geometry. Here we present a method for probing the current through a single C_{60} molecule while changing, one by one, the number of atoms in the electrode that are in contact with the molecule. We show quantitatively that the contact geometry has a strong influence on the conductance. We also find a crossover from a regime in which the conductance is limited by charge injection at the contact to a regime in which the conductance is limited by scattering at the molecule. Thus, the concepts of 'good' and 'bad' contacts, commonly used in macro- and mesoscopic physics, can also be applied at the molecular scale.

The geometry of a molecular junction is usually inferred indirectly from conductance data, and uncertainties related to the details of the molecule–electrode contacts have been circumvented by focusing on the length dependence of molecular wires[6] or by using well-defined anchoring chemistry[7]. The scanning tunnelling microscope (STM) can be used to make contacts with molecules[8,9] in a well-defined manner. Thus, the roles of molecular orientation[10], of submolecular variations of the contact position[11], and of progressive dehydrogenation of a molecule[12] have been explored directly in STM experiments. Nevertheless, the influence of the atomic-scale geometry of the contact on conductance has not been studied in detail, even though it is relevant to all molecular junctions. Here we explore the impact of atomic-scale geometry on the charge transport properties of C_{60}, which is a promising anchoring unit for molecular wires[13].

Using standard procedures[14], single copper atoms were deposited from an STM tip onto a Cu(111) surface and manipulated, one by one, to form clusters with atomically precise dimensions[15,16]. The STM image in Fig. 1a was acquired with a copper-terminated tip and shows clusters of N copper atoms (denoted Cu_N, where $N = 1, \ldots, 4$) that have been assembled by the lateral manipulation of the atoms deposited on the surface. Although linear arrangements of atoms were routinely obtained, the clusters occasionally adopted a two-dimensional compact shape during their formation[16]. Figure 1b shows an STM image recorded over the same sample area with a C_{60}-terminated tip[17]. The complex patterns observed on the atomic clusters correspond to 'reverse' images of the molecular tip, and reveal that one of the hexagons of the C_{60} cage is facing the surface. This atom-by-atom approach provides unprecedented control over the interface between the C_{60} molecule and one electrode (the copper atoms on the surface). Although we have less control over the geometry of the interface between the molecule and the other electrode (the tip), our experiments were conducted such that this interface remained unchanged over a series of measurements.

In a sequence of tip approaches a single C_{60} tip was first used to contact the pristine copper surface and then each atomic cluster. Typical conductance traces recorded during these approaches of a C_{60} tip to clusters with $N = 1, \ldots, 5$ are shown in Fig. 2a. After contact measurements at the clusters, yet another contact to the bare surface was made. Finally, images of the clusters were recorded to confirm that the molecular tip and the clusters had remained unchanged over the entire data acquisition process. This control procedure disclosed a systematic rearrangement of linear clusters to two-dimensional structures after the approach of a C_{60} tip and, in some cases, revealed a displacement of Cu_1 and Cu_2 (Fig. 2b–e). Only conductance data where both the molecular tip and the sample remained unchanged during a complete contact sequence will be discussed below.

In Fig. 2a, the right part of the traces corresponds to the tunnelling range. The inflection of the conductance curves is characteristic

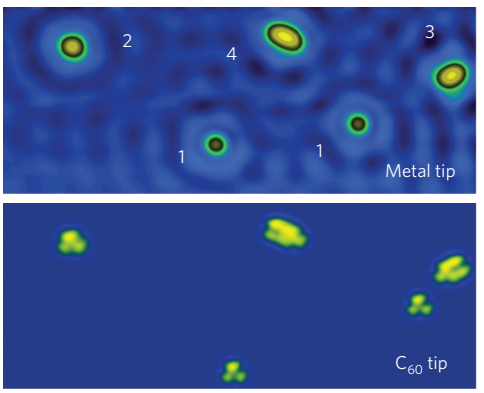

Figure 1 | STM images of atomically engineered electrodes on Cu(111). **a**, Constant-current STM image of Cu_N clusters on a Cu(111) surface obtained with a copper-terminated STM tip ($I = 0.1$ nA; sample voltage $V_s = 0.1$ V). **b**, Image obtained with a C_{60}-terminated STM tip ($I = 0.1$ nA; $V_s = -1.7$ V). The Cu_N clusters work as tips for 'reverse imaging' of the C_{60} fixed at the tip apex[17]. The threefold symmetric patterns reveal that one of the hexagons of the C_{60} cage is facing the surface. Standing waves related to surface states are not visible at this sample voltage. Both images, 18.2 nm × 7.2 nm.

[1]Institut de Physique et Chimie des Matériaux de Strasbourg, UMR 7504 (CNRS – Université de Strasbourg), 67034 Strasbourg, France, [2]Donostia International Physics Center (DIPC), 20018 San Sebastián, Spain, [3]Centro de Fisica de Materiales CSIC-UPV/EHU, Materials Physics Center MPC, 20080 San Sebastián, Spain, [4]Depto. Fisica de Materiales UPV/EHU, Facultad de Quimica, 20080 San Sebastián, Spain, [5]Institut für Experimentelle und Angewandte Physik, Christian-Albrechts-Universität zu Kiel, 24098 Kiel, Germany. *e-mail: guillaume.schull@ipcms.u-strasbg.fr; thomas_frederiksen@ehu.es

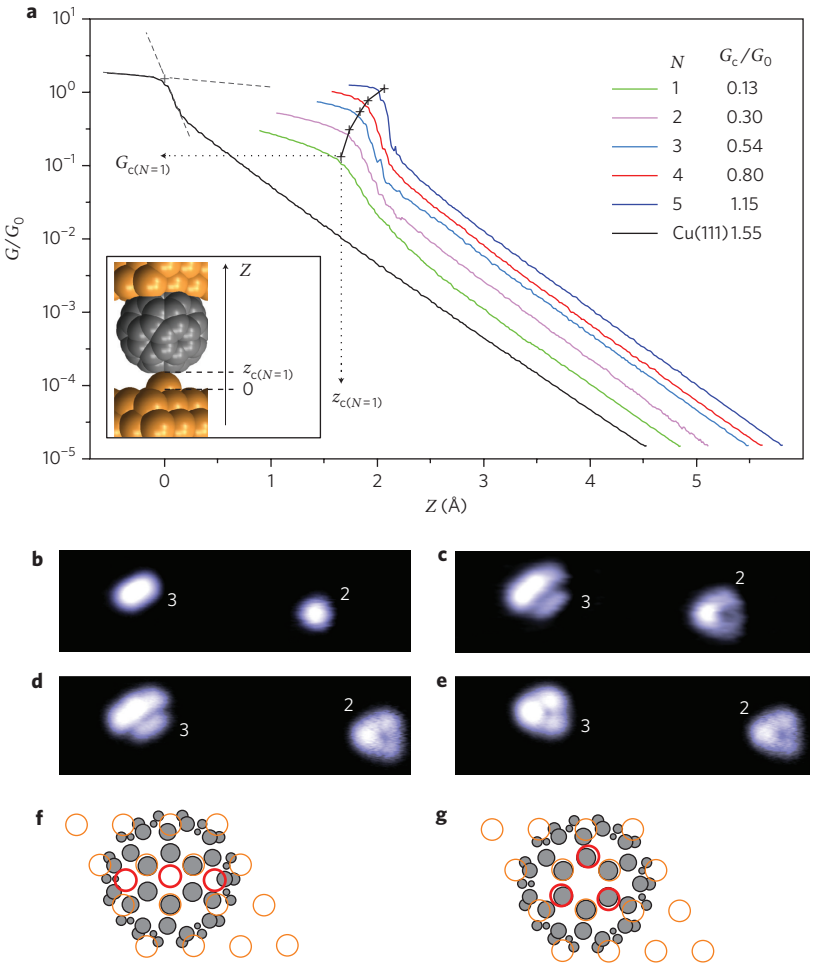

Figure 2 | Transport measurements of a single C_{60} molecule in contact with an increasing number of atoms. a, Conductance in units of G_0 (on a logarithmic scale) versus distance for a C_{60} tip approaching a bare Cu(111) surface (black line) and a surface covered with Cu_N clusters (coloured lines). One of the hexagons of the C_{60} cage is facing the surface. The distance scale was established from the apparent height of each cluster in STM images recorded at $I = 100$ pA and $V_s = -0.1$ V. Hereafter, with the same settings, the STM feedback was opened for collecting conductance data. Crosses mark the experimental contact points defined as the intersection of the contact and transition regimes (dashed grey lines indicate the bare surface data). Insets: geometry (bottom left) and list (right) of the experimental conductances at contact (G_c) derived from the conductance traces. z_c is the contact distance. **b**, STM image ($I = 100$ pA; $V_s = 0.1$ V; 8.0×2.3 nm^2) of Cu_2 and linear Cu_3 recorded with a copper tip. **c**–**e**, STM images ($I = 100$ pA; $V_s = -0.1$ V; 8.0×2.3 nm^2) of the same area recorded with a C_{60} tip. After the image in **c** was recorded, the approach of the C_{60} tip caused the Cu_2 cluster to move ~1.3 nm to the right (**d**), after which the approach of the tip to the linear Cu_3 cluster caused it to adopt a more compact configuration (**e**). **f**,**g**, Simulation showing how a linear Cu_3 (**f**, red circles) relaxes into a triangular configuration (**g**) as the distance between a C_{60} tip and the surface is reduced from 18 Å to 17.2 Å. The orange circles represent the Cu(111) surface; the carbon atoms are shown in grey.

of contact formation and defines the conductance at contact, G_c, and the contact distance z_c (ref. 18). The origin of the abscissa ($z = 0$) is set to z_c of the bare surface. Therefore, for $N = 1, \ldots, 5$, z_c is the z-position of the C_{60} tip in contact with the atomic cluster relative to the underlying surface (see inset to Fig. 2a). The data show an increase of z_c with the number of atoms in the cluster. This trend was observed in most cases and, as confirmed by our first-principles calculations, could be attributed to the progressive elongation of the cluster-surface bonds as the coordination of the cluster atoms increases.

Figure 3a summarizes a series of conductances at contact observed with C_{60} tips, exposing a hexagon to the copper sample. Their azimuthal orientation with respect to the clusters, however, varied. The highest contact conductance was always observed at the bare copper surface and varied from $1.0G_0$ to $1.6G_0$ ($G_0 = 2e^2/h$ is the conductance quantum) with different C_{60} tips. This variation probably also reflects differences in the inaccessible tip–molecule geometry. The significantly higher values than for C_{60} contacted with a sharp metallic tip[10] confirm that multiple atomic contacts must be present at the tip side. As shown in the figure, the conductance $G_c(N)$ is normalized to the conductance measured at the clean surface with the same tip to enable a comparison of the different series (the unprocessed data are shown in Supplementary Fig. S1). For all data sets $G_c(N)$ increases with N. When the conductance normalized by the number of cluster atoms is plotted against the number of atoms (that is, $G_c(N)/N$ versus N), a subtle maximum can be observed around $N \approx 5$ (Fig. 3b).

To further interpret the experimental observations we performed electronic structure calculations (see Methods) for supercells such as the one shown in Supplementary Fig. S2. Relaxed structures representing the experimental junctions were considered for two different electrode separations ($L_1 = 17.2$ Å and $L_2 = 18.0$ Å measured between the second-topmost electrode layers), corresponding to different molecule–cluster interaction regimes around the point of contact (details of the junction geometries are shown in Supplementary Figs S3 and S4). In these simulations, the bare Cu(111) surface is

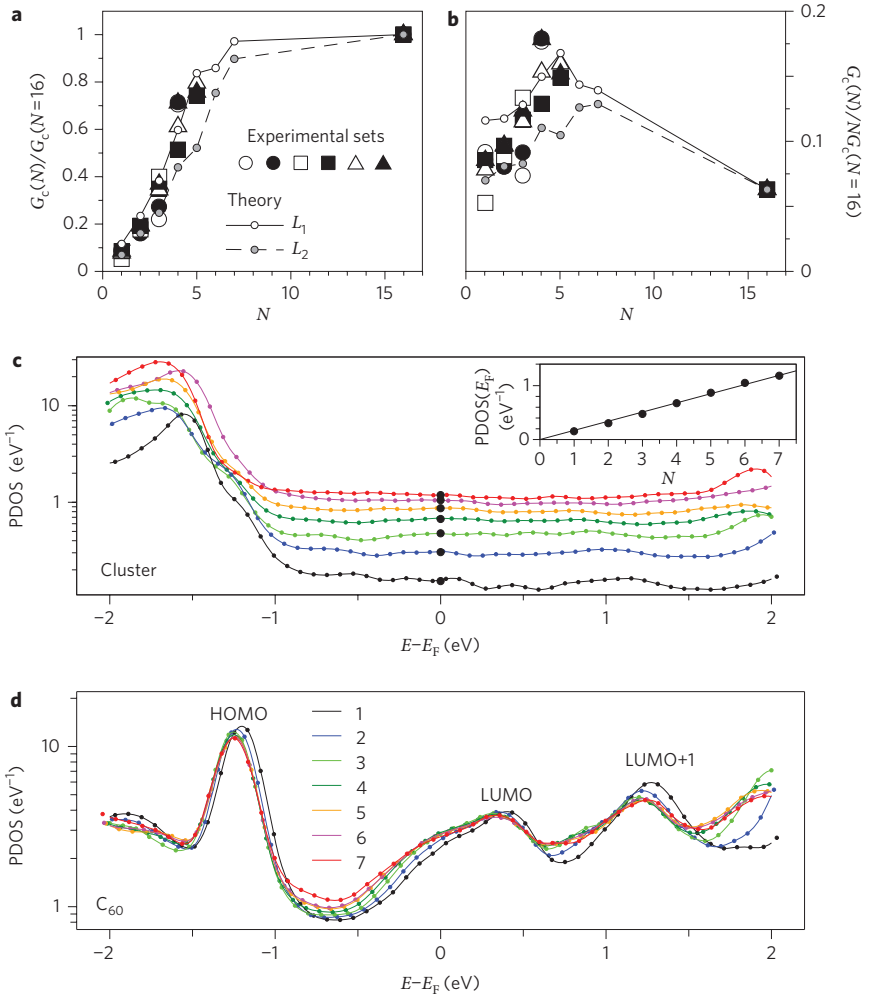

Figure 3 | Conductances at contact between a single C_{60} molecule and clusters of copper atoms. a, Normalized conductance at contact versus cluster size *N*. Experimental data from six different molecular tips are shown, as well as theoretical data for two electrode separations around the point of contact ($L_1 = 17.2$ Å and $L_2 = 18.0$ Å, measured between the second-topmost layers). Conductance is normalized to the value for a single C_{60} molecule in contact with a 16-atom cluster. **b**, Normalized conductance at contact per atom in the cluster versus cluster size *N*. **c**,**d**, Calculated PDOS onto the atomic basis orbitals (*s*, *p* and *d* character) of Cu_N (**c**) and C_{60} (**d**) versus energy for seven different cluster sizes and for a separation of $L_1 = 17.2$ Å. Inset to **c**: the PDOS of Cu_N at the Fermi energy varies linearly with *N*.

represented by a 4×4 array of copper atoms (that is, $N = 16$). We first discuss the evolution of the geometry of the junction at contact, in particular the rearrangement of linear clusters to two-dimensional structures upon contact with the C_{60} tip. This behaviour is reproduced by our simulations. Although cluster atoms can be arranged in any desired hollow-site pattern for the larger electrode separation (L_2), we found that bringing the tip 0.8 Å closer to the cluster (L_1) caused significant rearrangements. For instance, a linear trimer configuration would relax into a triangular two-dimensional arrangement (cf. Fig. 2f,g). This demonstrates that, close to contact, the interaction between the electrodes is strong enough to modify the atomic arrangement of the cluster. This effect is remarkable in its own right, but it may also explain some of the scatter of the data in Fig. 3, which were obtained with various C_{60} tips on various clusters.

We next turn to the influence of the number of copper adatoms on contact conductance. As seen in Fig. 3a, G_c increases with *N* in all experimental data sets, as well as in theory. This can be understood by considering that the number of quantum channels in an atomic-scale junction can be related to the number of valence orbitals in the constriction[19]. Thus, when the cluster cross-section is limiting the conductance it is expected to scale with *N*. More precisely, for a constant molecule–cluster distance, the injection rate of electrons into the molecular resonance is effectively determined by the density of states at the cluster at E_F (cf. Fig. 3c). When *N* is sufficiently large, however, the conductance at contact shows little variation with *N*, suggesting another origin of the transport limitation (to be discussed below).

The conductance per atom, G_c/N, versus cluster size *N* (Fig. 3b) has a maximum at $N \approx 5$. For small *N*, the rise of G_c/N indicates a growth of the conductance at contact with *N* steeper than linear. This super-linear effect is the result of the addition of two contributions: the aforementioned scaling with the cluster projected density of states (PDOS) (Fig. 3c) and modifications in the molecular resonances (Fig. 3d). In particular, with many atomic connections the lowest unoccupied molecular orbital (LUMO)-derived resonance of C_{60} shifts closer to E_F and also becomes broader due to an enhanced coupling to metal states. For large *N*, the decrease in G_c/N indicates a transition to the transport regime, where the conductance is limited only by the positions and hybridizations of the molecular resonances. Further analysis of the electronic structure shows a $2 + 1$ splitting of the threefold degenerate LUMO states of the free C_{60}, thereby explaining why the observed conductance in the contact approaches two (and not three) times the conductance quantum G_0.

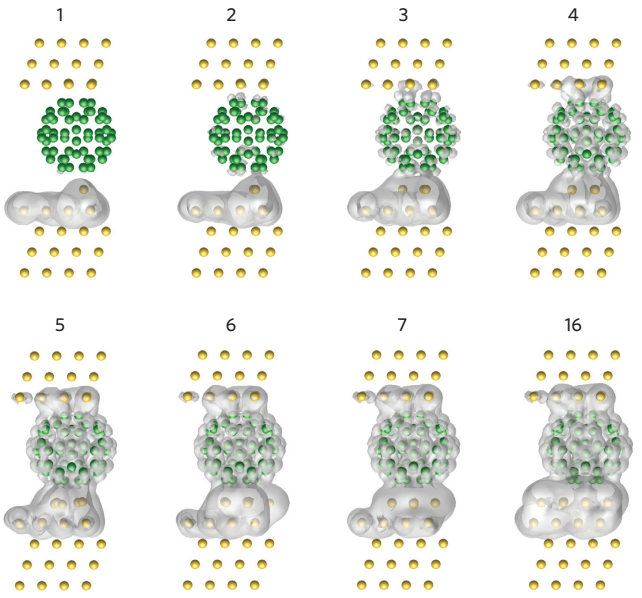

Figure 4 | Scattering at the contact between a single C_{60} molecule and clusters of copper atoms. Visualization of the scattering states at the Fermi energy for different numbers of contacting atoms. The calculated isosurfaces (shown in grey) represent the electron density in the junction at the centre of the Brillouin zone for a sum over the first three (most transmitting) eigenchannels (electron waves coming from below)[20]. Data were calculated for clusters with $N = 1, \ldots, 7$ and 16 adatoms at an electrode separation $L_1 = 17.2$ Å (measured between the second-topmost layers). Not all copper atoms in the cluster are visible. The scattering states are only calculated in the region of space defined by the topmost copper surface layers.

To understand the gradual evolution of the conductance per atom with N it is useful to visualize the electron density corresponding to the scattering states around the Fermi energy that are transmitted through the junction. These states characterize the electron transport through the transmission eigenchannels[20]. Isosurfaces of the electron density are shown in Fig. 4 (electron waves impinging from below) for a sum over the first three (most transmitting) eigenchannels, together with the atomic structure of the junctions (the individual eigenchannels are visualized in Supplementary Fig. S5). For $N = 1$, the incoming waves are strongly reduced at the single atom contact to the molecule, which acts as a bottleneck for electron transport. As N increases, the density at the bottom metal–molecule interface gradually increases (corresponding to a larger part of the waves being transmitted). At $N \approx 5$, the electron density plots do not single out a specific part of the junction as a limiting bottleneck. Instead, the molecular orbitals near the Fermi level control the number of transmission eigenchannels, and conductance is limited by scattering at the molecule. A further increase in the number of atomic connections to the molecule does not significantly affect the conductance, which explains why G_c/N decreases with N in this range. This also confirms that the tip–molecule interface, where a large number of connections is expected[17], plays little role in the variation of G_c with N. Finally, the maximum in the conductance per atom at $N \approx 5$ marks the crossover between cluster-size-limited ('bad contact' to the molecule) and molecule-limited ('good contact') transport regimes.

In summary, conductances have been reported for C_{60} molecules contacting metallic electrodes that are, for the first time, controlled at the level of individual atoms. The conductance of a C_{60} molecule varies by a factor of up to ~20, depending on the cross-section of the electrodes, illustrating that the conductance is not an intrinsic property of a molecule. Moreover, it might soon be possible to tune the transport properties of molecular junctions by controlling the positions and chemical natures of the atoms in the contacts.

Methods

Imaging and contact experiments were performed using a homemade ultrahigh vacuum (UHV) STM operated at 5 K. Cu(111) single-crystal surfaces and tungsten etched tips were prepared by Ar^+ bombardment and annealing cycles. As a last step of preparation, tungsten tips were repeatedly indented (by 1–5 nm) into clean areas of the copper samples to coat the tip apex with a thin layer of copper. C_{60} molecules were sublimated in UHV and deposited with submonolayer coverages on the Cu(111) surfaces at room temperature. C_{60}-terminated tips were obtained as described in ref. 17.

Theoretical calculations were performed with the SIESTA[21] pseudopotential density functional theory method as described in ref. 17. The electronic structure from SIESTA was used to calculate the transport properties for the TranSIESTA[22] setup. Relaxed structures that represent the experimental junctions were obtained in the following way. An initial structure consisting of a C_{60} molecule adsorbed with a hexagon on a hexagonal close-packed (hcp) hollow site on a 4×4 representation of a slab containing seven Cu(111) layers was fully relaxed, until all forces on the molecule and the surface layer were smaller than 0.02 eV/Å. Based on this configuration, larger supercells were built with 13 layers in the slab and N atoms positioned on the reverse side of the film. These adatoms and the underlying surface layer were then relaxed to 0.02 eV/Å for the two different electrode separations L_1 and L_2 (see main text). The PDOS was calculated using $20 \times 20 \times 1$ k-points and 0.1 eV broadening. The zero-bias conductance $G = G_0\, T(E_F)$ was derived from the transmission function $T(E_F)$ at the Fermi energy E_F, sampled over a 6×6 $\boldsymbol{k}_{||}$-mesh.

Received 2 September 2010; accepted 7 October 2010; published online 14 November 2010

References

1. Scott, J. C. Metal–organic interface and charge injection in organic electronic devices. *J. Vac. Sci. Technol. A* **21,** 521–531 (2003).
2. Nemec, N., Tománek, D. & Cuniberti, G. Contact dependence of carrier injection in carbon nanotubes: an ab initio study. *Phys. Rev. Lett.* **96,** 076802 (2006).
3. Basch, H., Cohen, R. & Ratner, M. A. Interface geometry and molecular junction conductance: geometric fluctuation and stochastic switching. *Nano Lett.* **5,** 1668–1675 (2005).
4. Xue, Y. & Ratner, M. A. Microscopic study of electrical transport through individual molecules with metallic contacts. ii. effect of the interface structure. *Phys. Rev. B* **68,** 115407 (2003).
5. Moth-Poulsen, K. & Bjørnholm, T. Molecular electronics with single molecules in solid-state devices. *Nature Nanotech.* **4,** 551–556 (2009).
6. Ho Choi, S., Kim, B. & Frisbie, C. D. Electrical resistance of long conjugated molecular wires. *Science* **320,** 1482–1486 (2008).
7. Quek, S. Y. *et al.* Mechanically controlled binary conductance switching of a single-molecule junction. *Nature Nanotech.* **4,** 230–234 (2009).
8. Joachim, C., Gimzewski, J. K., Schlittler, R. R. & Chavy, C. Electronic transparence of a single C_{60} molecule. *Phys. Rev. Lett.* **74,** 2102–2105 (1995).
9. Schulze, G. *et al.* Resonant electron heating and molecular phonon cooling in single C_{60} junctions. *Phys. Rev. Lett.* **100,** 136801 (2008).
10. Néel, N., Kröger, J., Limot, L. & Berndt, R. Conductance of oriented C_{60} molecules. *Nano Lett.* **8,** 1291–1295 (2008).
11. Temirov, R., Lassise, A., Anders, F. B. & Tautz, F. S. Kondo effect by controlled cleavage of a single-molecule contact. *Nanotechnology* **19,** 065401 (2008).
12. Wang, Y. F. *et al.* Atomic-scale control of electron transport through single molecules *Phys. Rev. Lett.* **104,** 176802 (2010).
13. Martin, C. A. *et al.* Fullerene-based anchoring groups for molecular electronics. *J. Am. Chem. Soc.* **130,** 13198–13199 (2008).
14. Limot, L., Kroger, J., Berndt, R., Garcia-Lekue, A. & Hofer, W. A. Atom transfer and single-adatom contacts. *Phys. Rev. Lett.* **94,** 126102 (2005).
15. Repp, J., Meyer, G., Rieder, K.-H. & Hyldgaard, P. Site determination and thermally assisted tunneling in homogenous nucleation. *Phys. Rev. Lett.* **91,** 206102 (2003).
16. Fölsch, S., Hyldgaard, P., Koch, R. & Ploog, K. H. Quantum confinement in monatomic Cu chains on Cu(111). *Phys. Rev. Lett.* **92,** 056803 (2004).
17. Schull, G., Frederiksen, T., Brandbyge, M. & Berndt, R. Passing current through touching molecules. *Phys. Rev. Lett.* **103,** 206803 (2009).
18. Néel, N. *et al.* Controlled contact to a C_{60} molecule. *Phys. Rev. Lett.* **98,** 065502 (2007).
19. Scheer, E. *et al.* The signature of chemical valence in the electrical conduction through a single-atom contact. *Nature* **394,** 154–157 (1998).

20. Paulsson, M. & Brandbyge, M. Transmission eigenchannels from nonequilibrium Green's functions. *Phys. Rev. B* **76,** 115117 (2007).
21. Soler, J. M. *et al*. The SIESTA method for ab initio order-*n* materials simulation. *J. Phys. Condens. Matter* **14,** 2745–2779 (2002).
22. Brandbyge, M., Mozos, J. L., Ordejon, P., Taylor, J. & Stokbro, K. Density-functional method for nonequilibrium electron transport. *Phys. Rev. B* **65,** 165401 (2002).

Acknowledgements

This work was supported by the Deutsche Forschungsgemeinschaft (SFB 677), the Schleswig–Holstein Fonds, the Ministerio de Cienciae Innovacion (FIS2007-6671) and the Basque Department of Education (IT-366-07).

Author contributions

G.S. and R.B. provided the experimental concept. G.S. performed the STM and contact experiments. T.F. performed the first-principles calculations, and analysis was carried out with A.A. and D.S.P. All authors contibuted to the discussion of the results and preparation of the manuscript.

Additional information

The authors declare no competing financial interests. Supplementary information accompanies this paper at www.nature.com/naturenanotechnology. Reprints and permission information is available online at http://npg.nature.com/reprintsandpermissions/. Correspondence and requests for materials should be addressed to G.S. and T.F.